Meteoritics & Planetary Science 39, Nr 3, 387–399 (2004)
Abstract available online at http://meteoritics.org

Devgaon (H3) chondrite: Classification and complex cosmic ray exposure history

S. V. S. MURTY,[1*] V. K. RAI,[1] A. D. SHUKLA,[1] G. SRINIVASAN,[1] P. N. SHUKLA,[1] K. M. SUTHAR,[1] N. BHANDARI,[1] and A. BISCHOFF[2]

[1]Planetary and Geosciences Division, Physical Research Laboratory, Ahmedabad 380009, India
[2]Institut für Planetologie, Wilhelm-Klemm-Strasse 10, D-48149 Münster, Germany
[*]Corresponding author. E-mail: murty@prl.ernet.in

(Received 3 February 2003; revision accepted 8 December 2003)

Abstract–The Devgaon meteorite fell in India on February 12, 2001 and was immediately collected. It is an ordinary chondrite having a number of SiO_2-rich objects and some Ca, Al-rich inclusions. Olivines (Fa_{17-19}) are fairly equilibrated, while pyroxenes (Fs_{4-20}) are unequilibrated. Occasionally, shock veins are visible, but the bulk rock sample is very weakly shocked (S2). Chondrules and chondrule fragments are abundant. Based on chemical and petrological features, Devgaon is classified as an H3.8 group chondrite. Several cosmogenic radionuclides ranging in half-lives from 5.6 d (^{52}Mn) to 7.3×10^5 yr (^{26}Al), noble gases (He, Ne, Ar, Kr, and Xe), and particle track density have been measured. The track density in olivines from five spot samples varies between (4.6 to 9) × 10^6 cm^{-2} showing a small gradient within the meteorite.

The light noble gases are dominated by cosmogenic and radiogenic components. Large amounts of trapped gases (Ar, Kr, and Xe) are present. In addition, (n, γ) products from Br and I are found in Kr and Xe, respectively. The average cosmic ray exposure age of 101 ± 8 Ma is derived based on cosmogenic ^{38}Ar, ^{83}Kr, and ^{126}Xe. The track production rates correspond to shielding depths of about 4.9 to 7.8 cm, indicating that the stone suffered type IV ablation. Low ^{60}Co, high (^{22}Ne/^{21}Ne)$_c$, and large neutron produced excesses at ^{80}Kr, ^{82}Kr, and ^{128}Xe indicate a complex exposure history of the meteoroid. In the first stage, a meter-sized body was exposed for nearly 10^8 yr in the interplanetary space that broke up in ~50 cm-sized fragments about a million years ago (stage 2), before it was captured by the Earth.

FALL, PETROGRAPHY, AND MINERALOGY

A single stone weighing about 12 kg fell in the village of Devgaon, Bastar district, Chattisgarh, Central India on February 12, 2001 at about 16:00 hours IST. The meteorite was fully covered with fusion crust (Fig. 1) at the time of recovery. The meteorite was quickly recovered and delivered to the district Collectorate from whom one of us (G. Srinivasan) got a piece weighing about 3.8 kg.

Devgaon is an ordinary chondrite consisting of abundant chondrules and chondrule fragments embedded within a moderately recrystallized fine-grained matrix (Fig. 2). Studies of thin sections show that most constituents of the meteorite are fragmented. In contrast, the hand specimen of Devgaon looks quite homogeneous without any indication of brecciation. Occasionally, shock veins are visible (Fig. 3), although the bulk rock is very weakly shocked and is classified as shock grade S2 (Stöffler et al. 1991). The Olivines show undulatory extinction and irregular fractures but no planar deformation. The multiple degrees of shock effects indicate that the event responsible for the formation of shock veins is not responsible for the fragmentation of the meteorite components. Therefore, we conclude that the process of fragmentation must have occurred before accumulation of the material on the parent body from which the Devgaon meteoroid is derived. In thin section, many types of chondrules are observed, partly containing brownish mesostasis glass. In addition, some Ca, Al-rich inclusions (CAIs) were detected, which are mainly rich in Fe-rich spinel. One of these inclusions is shown in Fig. 4 and consists of abundant spinel and ilmenite. The spinel is zoned showing an increase of Cr and Zn toward the rim of the CAI. A Na-rich phase is located at the edge of the inclusion (Fig. 4). Similar CAIs were found in several other ordinary chondrites (Bischoff and Keil 1983, 1984). It appears that intense alteration has affected the original composition and mineralogy of the inclusions. As also suggested for the CAIs in ordinary chondrites (Bischoff and Keil 1984), ilmenite is most probably an alteration product of perovskite. During alteration, CaO was replaced by FeO and MgO by FeO in

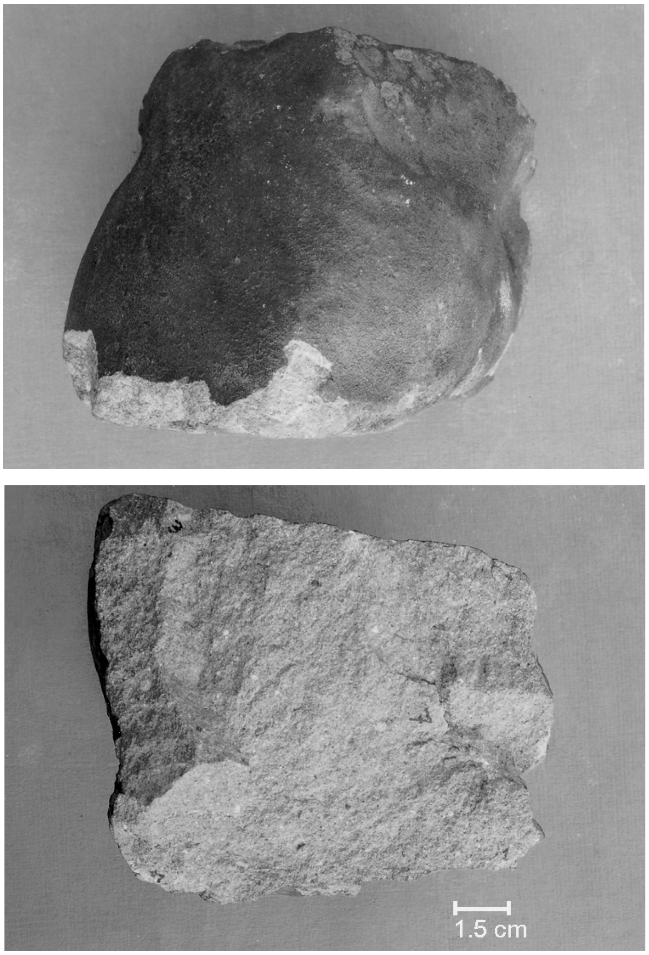

Fig. 1. The crusted and interior face of the Devgaon meteorite.

perovskite and spinel, respectively. Thin section studies show a considerable number of unusual SiO_2-rich objects. One example is shown in Fig. 5. It mainly consists of an SiO_2-phase and pyroxene. The chondrule-like object is surrounded by fine-grained olivine and pyroxene.

Most meteorite constituents in Devgaon have equilibrated olivine (Fa_{17-19}, range 4–19 mol% Fa); however, a small number of olivines have much lower Fa contents (Table 1). Based on the analyses of 37 olivine grains, an average value of 17.0 ± 2.2 mol% Fa was obtained. Based on the composition of olivine, the chondrite is classified as H3.8. Pyroxene is highly unequilibrated (Fs_{4-20}; Table 1). The analyses of 36 individual grains revealed an average of 10.9 ± 4.0 mol% Fs. This classification is consistent with the observation that ordinary chondrites with petrologic types close to 4 usually show olivines more equilibrated compared to pyroxenes.

CHEMICAL COMPOSITION

Interior chips (~4 g) were gently crushed to a fine bulk powder, and several major, minor, and trace elements were measured using ICP-AES (inductively coupled plasma atomic emission spectrometry), AAS (atomic absorption spectrometry), and INAA (instrumental neutron activation analysis). For ICP-AES and AAS, two aliquots (~200 mg each) from the bulk powder were sequentially treated with HF, HCl, and $HClO_4$ and, finally, were dissolved in dilute HNO_3. The Dhajala (H3.8) meteorite and rock standard diabase W-2 were used as standards. Several major elements (Fe, Ni, Al, Ca, Mg) were measured using ICP-AES, and K

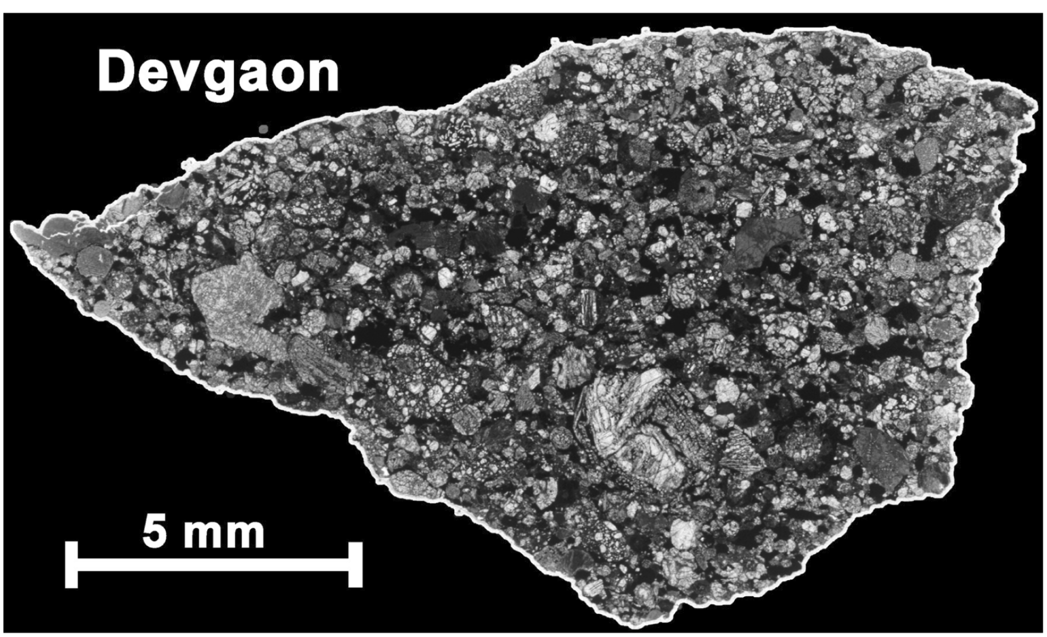

Fig. 2. A view of a thin section from Devgaon in transmitted light showing abundant chondrules.

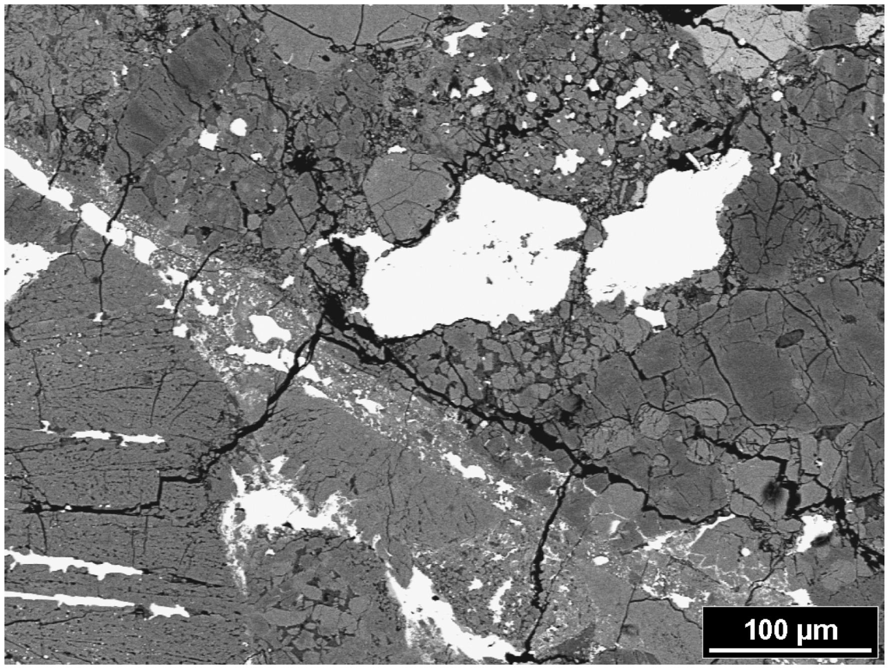

Fig. 3. Shock veins in Devgaon. This SEM image in backscattered electrons also shows abundant fractured objects.

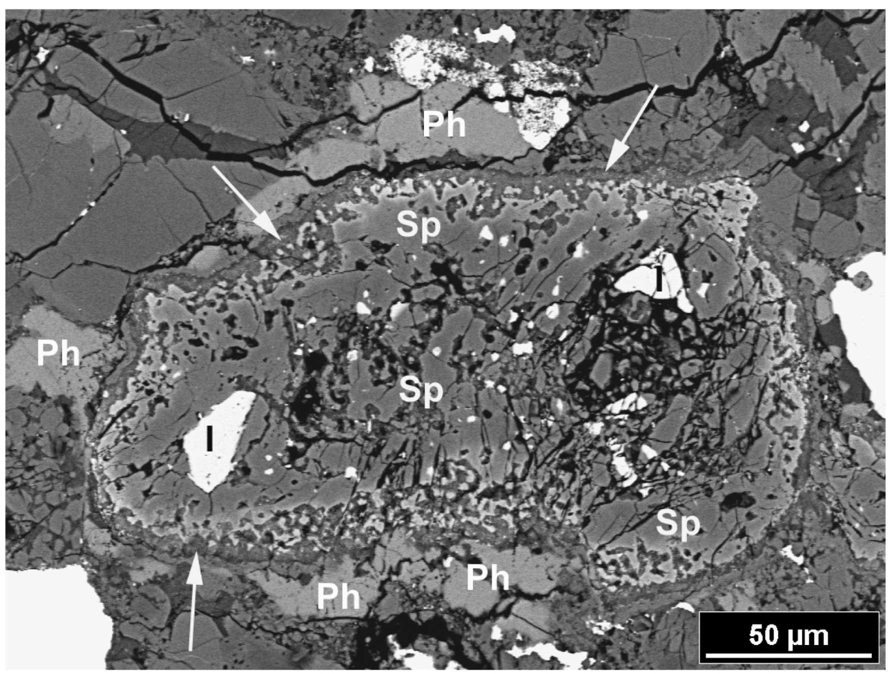

Fig. 4. Backscattered electron image showing Al-rich inclusions consisting of abundant spinel (Sp) and ilmenite (I). The spinel containing small grains of ilmenite (white) is zoned having an increase of Cr and Zn toward the rim of the CAI. A Na-rich phase is located at the edge of the inclusion (arrows). Some large phosphate grains (Ph) are located at the border.

was measured using AAS. Potassium measurements were also carried out using γ-ray spectrometry by comparing the 1.46 MeV γ-ray (from ^{40}K) intensity of the meteorite with that of a known standard (Basalt 107). INAA measurements were carried out in two separate irradiations. In each case, four aliquots (50 mg to 70 mg) from the bulk powder were irradiated with neutrons in the Dhruva reactor at the Bhabha Atomic Research Centre, Mumbai. The irradiated samples and standards were counted for their characteristic γ-rays at different intervals of time on a high purity Ge detector

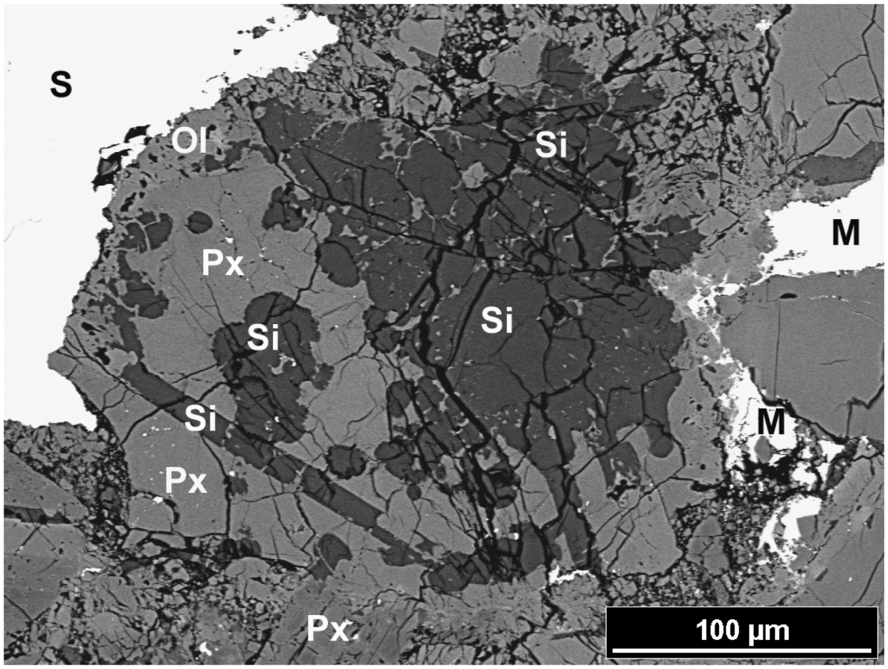

Fig. 5. Backscattered electron image showing an unusual SiO_2-rich object in the Devgaon chondrite mainly containing an SiO_2 phase (Si) and pyroxene (Px). The chondrule-like object is surrounded by fine-grained olivine (Ol) and pyroxene (Px). The latter is less FeO-rich than the pyroxene within the object. Metal (M) and sulfide (S) occur in the surroundings.

Table 1. Composition of representative olivines and pyroxenes within the Devgaon (H3.8) ordinary chondrite.

	Pyroxene					Olivine			
MgO	29.9	36.9	34.2	28.1	34.6	53.0	43.5	43.6	44.2
Al_2O_3	1.48	0.15	0.26	2.12	–	–	<0.07	–	<0.11
SiO_2	55.9	58.8	56.5	53.2	57.0	41.1	38.5	39.5	39.2
CaO	1.08	0.16	0.20	1.85	0.44	0.41	–	–	–
TiO_2	0.28	–	–	0.20	0.31	<0.20	<0.10	–	–
Cr_2O_3	<0.12	0.15	0.14	1.36	0.59	0.21	<0.05	–	<0.05
MnO	0.80	0.14	0.53	<0.10	0.18	0.19	0.63	0.28	0.29
FeO	10.3	3.2	8.2	12.7	6.6	4.5	17.1	16.0	15.5
Fs/Fa	15.9	4.6	11.8	19.5	9.6	4.5	18.1	17.1	16.5

(148 cm^3) located in a 10 cm-thick lead shield following standard procedures (Laul 1979). In this way, the concentration of several elements such as Fe, Ni, Co, Cr, Na, Se, Zn, Sc, La, Sm, Eu, Yb, Ir, Os, and Au were determined. The weighted mean concentrations observed in various aliquots of the bulk meteorite are given in Table 2. As can be seen from Table 2, the values for siderophile elements including the platinum group elements (Fe, Co, Ni, Ir, Os, and Au) match well with those of the H class of ordinary chondrites (Kallemeyn et al. 1989).

NOBLE GASES

A clean chip of the meteorite, part of which was used for chemical analysis, has been used for noble gas studies. The sample was wrapped in Al foil and loaded into the extraction system of the noble gas mass spectrometer. All noble gases were analyzed by stepwise pyrolysis, after an initial combustion at 400 °C in 2 torr O_2, using standard procedures described earlier (Murty 1997; Murty et al. 1998). The data reported here have been corrected for blanks, interferences, and instrumental mass discrimination. Blanks at all temperatures are ≤5% of the signal and have near atmospheric isotopic composition within errors. The results of the measurements of He, Ne, and Ar are given in Table 3, while Kr and Xe data are compiled in Table 4 and Table 5, respectively. ^{78}Kr data are not reported due to large background contribution at mass 78. He and Ne consist of almost pure cosmogenic and radiogenic (^4He) components, while Ar, Kr, and Xe are dominated by trapped component with small contributions from cosmogenic and radiogenic components.

Using the end member compositions suggested by Eugster (1988) for trapped and cosmogenic components in

Table 2. Chemical composition of the Devgaon chondrite.[a]

Element	Concentration
Al (%)	1.11
Ca (%)	1.11
Mg (%)	13.5
Fe (%)	26.6
Ni (%)	1.75
Co (ppm)	820
Cr (ppm)	3875
Na (ppm)	7201
K (ppm)	804
Zn (ppm)	60.6
Se (ppm)	8.3
Sc (ppm)	8.4
La (ppm)	0.40
Sm (ppm)	0.22
Eu (ppm)	0.10
Yb (ppm)	0.29
Ir (ppb)	824
Os (ppb)	824
Au (ppb)	170

[a]Errors for major elements are ≤2% except for Ca (5%). For trace elements, errors are still ≤10% and represent 1σ statistical counting errors for elements determined for INAA, except for Os where the error is 20%.

ordinary chondrites, we have derived cosmogenic ^{3}He, ^{21}Ne, ^{38}Ar, ^{83}Kr, and ^{126}Xe and radiogenic (^{4}He, ^{40}Ar) components. These are given in Table 6a. We will first discuss the radiogenic and nucleogenic components.

Radiogenic Components and Gas Retention Ages

From the radiogenic ^{4}He and ^{40}Ar (Table 6a) and the average U (12 ppb) and Th (42 ppb) contents of H chondrites (Wasson and Kallemeyn 1988) and K (804 ppm) content of Devgaon (Table 2), we derive nominal U, Th-^{4}He (T_4) and K-Ar (T_{40}) ages of 3.99 ± 0.40 and 4.6 ± 0.46 Ga, respectively. Both these ages are in agreement within error limits and suggest almost quantitative retention of radiogenic ^{4}He and ^{40}Ar. This indicates that there has been no major thermal or shock events leading to significant loss of radiogenic ^{4}He and ^{40}Ar. The event leading to the formation of shock viens (Fig. 3) must have occurred very early on the Devgaon parent body.

Nucleogenic Component

Isotopic data of Kr show significant excesses at ^{80}Kr and ^{82}Kr, over and above that expected due to spallation, as

Table 3. Light noble gases in the Devgaon meteorite (Sample wt. = 506.24 mg).[a]

Temp. (°C)	^{4}He (10^{-8} ccSTP/g)	^{22}Ne	^{36}Ar	^{3}He/^{4}He (×10^{4})	^{20}Ne/^{22}Ne	^{21}Ne/^{22}Ne	^{38}Ar/^{36}Ar	^{40}Ar/^{36}Ar
400	8.6	0.025	0.063	600.8 ± 50.8	0.8476 ± .0254	0.8109 ± .0059	0.1885 ± .0012	45.7 ± .4
1000	1806	8.68	1.84	348.1 ± 29.5	0.8415 ± .0005	0.8305 ± .0004	0.6903 ± .0011	2744 ± 53
1200	101.2	6.01	5.48	285.4 ± 24.2	0.8423 ± .0006	0.8511 ± .0005	0.3427 ± .0006	222.0 ± 4.3
1600	18.6	3.08	4.91	545.5 ± 46.2	0.8444 ± .0009	0.8573 ± .0003	0.3306 ± .0002	76.8 ± 1.5
Total	1934	17.80	12.29	347.8 ± 29.4	0.8423 ± .0006	0.8421 ± .0004	0.3891 ± .0005	540.5 ± 10.5

[a]Errors in concentrations are ±10%. Errors in isotopic ratios represent 95% confidence limits.

Table 4. Krypton in the Devgaon meteorite.

Temp. (°C)	^{84}Kr (10^{-12} ccSTP/g)	^{80}Kr (^{84}Kr ≡ 100)	^{82}Kr	^{83}Kr	^{86}Kr
400	79	–	–	–	–
1000	103.7	22.97 ± .04	28.74 ± .14	23.58 ± .02	30.81 ± .24
1200	424.2	5.454 ± .040	21.06 ± .02	20.97 ± .06	30.79 ± .10
1600	406.2	4.492 ± .021	20.79 ± .07	20.61 ± .08	31.07 ± .05
Total	1013	6.980 ± 0.32	21.78 ± .06	21.04 ± .06	30.92 ± .09

Table 5. Xenon in the Devgaon meteorite

Temp. (°C)	^{132}Xe (10^{-12} ccSTP/g)	^{124}Xe (^{132}Xe ≡ 100)	^{126}Xe	^{128}Xe	^{129}Xe	^{130}Xe	^{131}Xe	^{134}Xe	^{136}Xe
400	116.2	0.4359 ± .0133	0.4842 ± .0063	8.332 ± .026	104.9 ± .2	16.08 ± .02	83.48 ± .06	38.21 ± .01	32.51 ± .05
1000	80.8	0.4923 ± .0150	0.5900 ± .0077	8.869 ± .057	281.9 ± .6	16.46 ± .05	82.55 ± .15	37.81 ± .01	31.58 ± .11
1200	327.2	0.5319 ± .0078	0.4710 ± .0083	8.395 ± .031	132.7 ± .3	16.31 ± .06	82.20 ± .09	37.84 ± .13	31.49 ± .07
1600	655.6	0.5028 ± .0045	0.4567 ± .0027	8.383 ± .034	117.7 ± .3	16.32 ± .03	82.15 ± .09	37.76 ± .02	31.38 ± .07
Total	1180	0.5035 ± .0070	0.4725 ± .0049	8.415 ± .034	131.9 ± .3	16.30 ± .04	82.32 ± .09	37.83 ± .05	31.53 ± .07

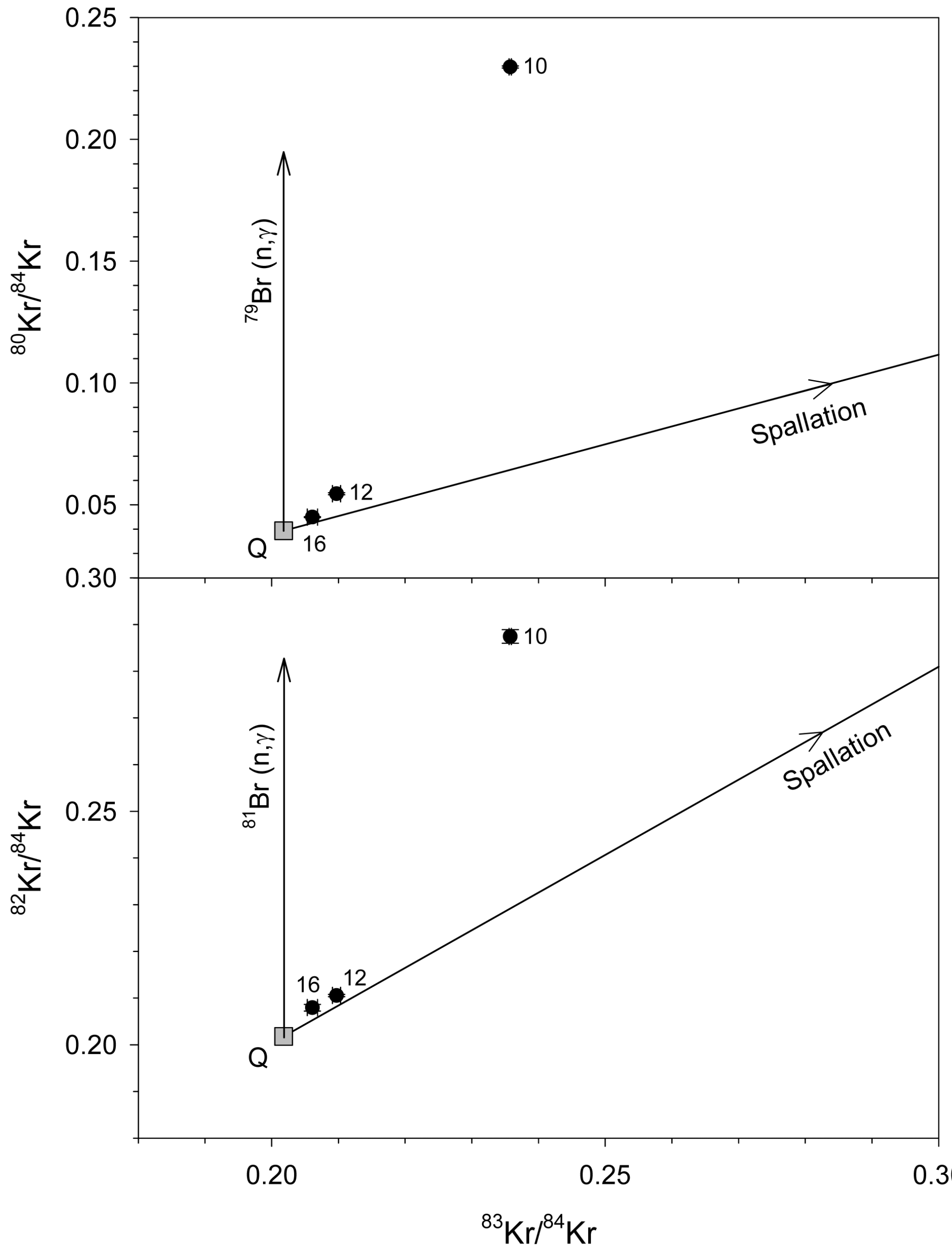

Fig. 6. ^{80}Kr/^{84}Kr and ^{82}Kr/^{84}Kr are plotted against the ^{83}Kr/^{84}Kr ratio. Trends expected for two component mixtures of spallation + trapped Kr and Br(n, γ) products + trapped Kr are also indicated in the plot. The numbers beside each point indicate temperature in 100s °C. Contributions from Br(n, γ) reactions, particularly in the 1000 °C fraction are clearly seen.

indicated by ^{83}Kr/^{84}Kr ratio. In Fig. 6 where the ratios ^{80}Kr/^{84}Kr and ^{82}Kr /^{84}Kr are plotted against ^{83}Kr /^{84}Kr, the data points do not follow the spallation line, but fall on the side of excess ^{80}Kr and ^{82}Kr. These excesses are most dominantly seen in the 1000 °C fraction, suggesting that these components are hosted in a volatile phase. Similarly, in the plot of ^{128}Xe/^{132}Xe against ^{126}Xe/^{132}Xe (Fig. 7), some data points fall above the spallation trend for H chondrites, indicating the presence of excess ^{128}Xe over and above that expected from spallation. Figure 7 also shows a good correlation between ^{128}Xe and ^{129}Xe (normalized to ^{132}Xe), relating the excess ^{128}Xe to I. As in the case of Kr, the most prominent shift in ^{128}Xe/^{132}Xe is in the 1000 °C fraction. About 70 (±5) percent of excess ^{82}Kr and ^{128}Xe are released in the 1000 °C fraction, as also the maximum release (48%) of ^{129}Xe* (^{129}Xe* = radiogenic ^{129}Xe due to ^{129}I decay). The similarity in release temperature and the parallel between

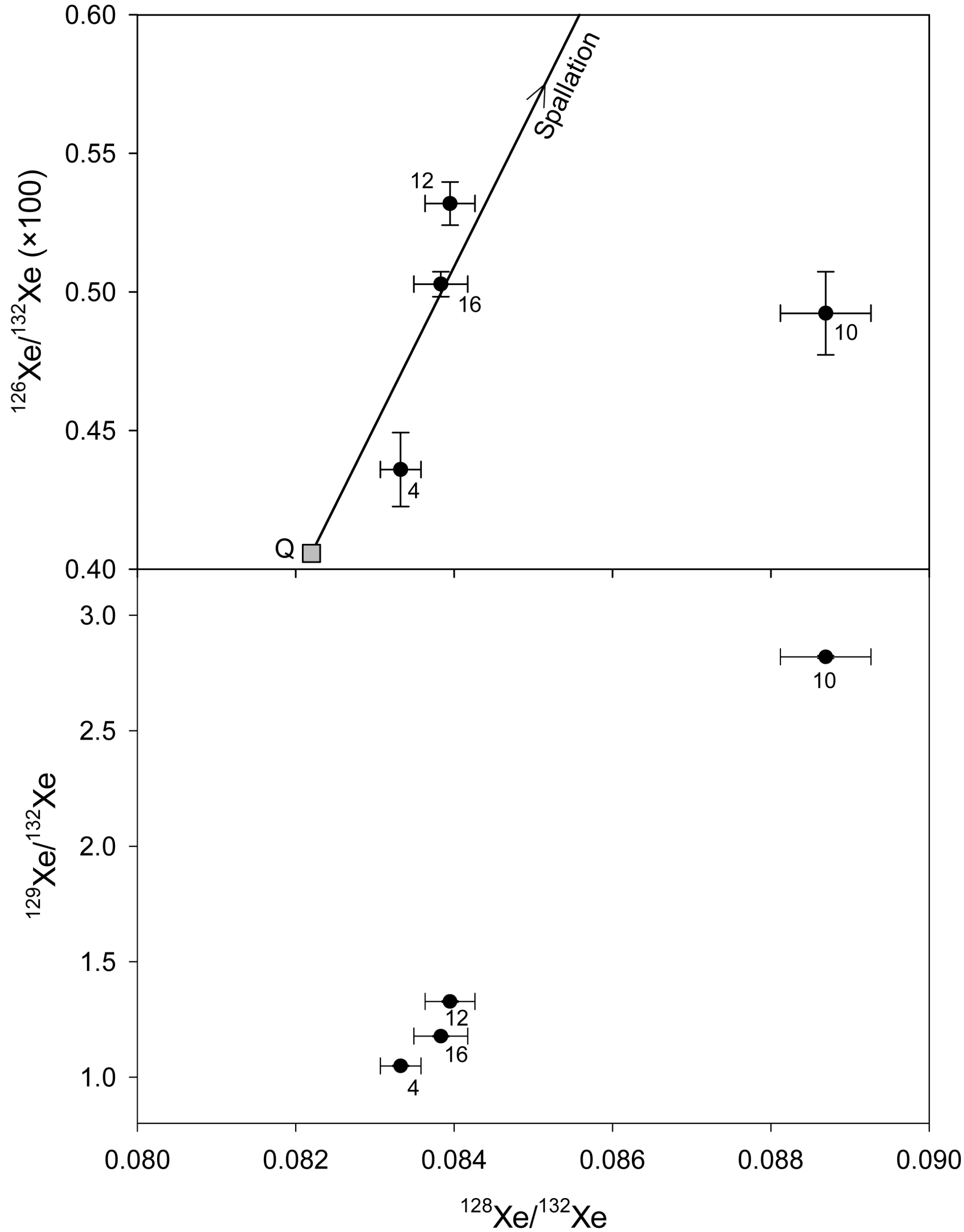

Fig. 7. $^{126}Xe/^{132}Xe$ and $^{129}Xe/^{132}Xe$ are plotted against $^{128}Xe/^{132}Xe$ showing the presence of the $^{127}I(n, \gamma)$ contribution. The 1000 °C point deviates from the spallation trend (top panel), indicating the contribution of ^{128}Xe from the (n, γ) reaction on ^{127}I. The good correlation between $^{128}Xe/^{132}Xe$ and $^{129}Xe/^{132}Xe$ (bottom panel) establishes that both are related to iodine.

the excesses at ^{80}Kr, ^{82}Kr, ^{128}Xe, and ^{129}Xe clearly point out that the source of the excesses is the (n, γ) reactions on Br and I.

The total excesses at ^{80}Kr, ^{82}Kr, ^{83}Kr, ^{126}Xe, and ^{128}Xe are calculated taking the trapped compositions of Kr and Xe as Q components (Busemann et al. 2000). As excesses of ^{126}Xe and ^{83}Kr are purely from spallation, using the spallation spectra of Kr (Lavielle and Marti 1988) and Xe (Hohenberg et al. 1981), the spallation contributions at ^{80}Kr, ^{82}Kr, and ^{128}Xe have been estimated and subtracted from the total excesses to derive the neutron produced amounts of $^{80}Kr_n$, $^{82}Kr_n$, and $^{128}Xe_n$, respectively from ^{79}Br, ^{81}Br, and ^{127}I through the (n, γ) reaction. These values are given in Table 6a. The ratio of $(^{80}Kr/^{82}Kr)_n = 2.44$ is closer to the value of 2.5 expected for neutron energies in the range of 30–300 eV. A value of about 3.3 is expected for thermal neutrons (Marti et al. 1966). In view of the above, a contribution to ^{36}Ar ($^{36}Ar_n$) is expected

Table 6a. Cogmogenic and nucleogenic components (in ccSTP/g units).

Cosmogenic					Nucleogenic			
^{3}He	^{21}Ne	^{38}Ar	^{83}Kr	^{126}Xe	^{36}Ar	^{80}Kr	^{82}Kr	^{128}Xe
10^{-8}			10^{-12}		10^{-8}	10^{-12}		
67.3	14.9	3.60	10.0	0.696	3.58	29.1	11.9	0.373

Table 6b. Radiogenic and trapped components (in ccSTP/g units).

Radiogenic		Trapped		
^{4}He	^{40}Ar	^{36}Ar	^{84}Kr	^{132}Xe
10^{-8}		10^{-8}	10^{-12}	
1584	6645	6.32	1007	1179

Table 6c. Cosmic ray exposure ages (Ma) and gas retention ages (Ga).[a]

Cosmic ray exposure ages					Gas retention ages	
T_3	T_{21}	T_{38}	T_{83}	T_{126}	T_4	T_{40}
43.4	63.8	88.4	103.5	110.7	3.99 ± .40	4.60 ± .46
Avg. (T_{38}, T_{83}, T_{126}) = 101 ± 8						

[a]Errors in T_3, T_{21}, and T_{38} are ±10%; T_{83} and T_{126} are ±15%.

from the $^{35}Cl(n, \gamma)$ reaction. We can not estimate $^{36}Ar_n$ from Ar data, which is essentially a two isotope (^{36}Ar, ^{38}Ar) system but a three component (trapped, cosmogenic, and nucleogenic) mixture. To estimate the amount of $^{36}Ar_n$, we use $^{82}Kr_n$. Assuming the (Cl/Br) atom ratio in Devgaon to be 700, the same as in average H chondrites (Mason 1979), and using (n, γ) cross sections from Göbel et al. (1982), we calculate $^{36}Ar_n = 3.58 \times 10^{-8}$ ccSTP/g.

Cosmogenic Components and Exposure Ages

Cosmogenic $(^{22}Ne/^{21}Ne)_c$ has a value of 1.182 ± 0.001, indicating shallow depth for the sample analyzed for noble gases. For the chemical composition of Devgaon and the shielding parameter as given by $(^{22}Ne/^{21}Ne)_c$, production rates are calculated for all noble gas isotopes, except for ^{38}Ar, following the procedure suggested by Eugster (1988). In the case of ^{38}Ar, the modified procedure of Marti and Graf (1992) has been used. The exposure ages obtained for various noble gas isotopes are (in Ma) $T_3 = 43.4$, $T_{21} = 63.8$, $T_{38} = 69.4$, $T_{83} = 103.5$, $T_{126} = 110.7$. Exposure ages based on ^{83}Kr and ^{126}Xe are in agreement within errors, but those based on ^{3}He, ^{21}Ne, and ^{38}Ar are substantially lower. Lower ages obtained from ^{3}He and ^{21}Ne could be due to partial loss of He, Ne during the long cosmic ray exposure. Diffusive loss of ^{3}H from metal and loss due to possible solar heating of ^{3}He and ^{21}Ne during the interplanetary sojourn of the meteoroid usually have been implicated as some of the causes for partial ^{3}He and ^{21}Ne losses found in meteorites (Hintenberger et al. 1966). The K-Ar age of 4.60 ± 0.46 Ga indicates a near total retention of ^{40}Ar in Devgaon, suggesting that the process, which resulted in partial loss of He and Ne, has not caused any measurable loss of Ar. Therefore, partial loss of ^{38}Ar is an unlikely explanation for the lower value of T_{38}. We infer that the low value of T_{38} is an artifact due to the presence of neutron-produced $^{36}Ar_n$ from the (n, γ) reaction on ^{35}Cl, which was not considered in the calculation of $^{38}Ar_c$. It is known that the presence of $^{36}Ar_n$, if ignored, results in an apparent lower estimate of $^{38}Ar_c$, resulting in lower T_{38} (Bogard et al. 1995; Wieler et al. 1996; Bhandari et al. 2002). We first estimate $^{36}Ar_n$ ($=3.58 \times 10^{-8}$ ccSTP/g) from $^{82}Kr_n$. We subtracted this practically mono-isotopic component from the total measured Ar and recalculated the $^{38}Ar_c = 3.60 \times 10^{-8}$ ccSTP/g (as compared to 2.82×10^{-8} ccSTP/g, obtained without correcting for $^{36}Ar_n$) and obtain $T_{38} = 88.4 \pm 9.0$ Ma. This value is in agreement with T_{83} and T_{126} within the uncertainties. Therefore, we adopt the mean value of T_{38}, T_{83}, and T_{126} of 101 ± 8 Ma as the cosmic ray exposure age of Devgaon. Among the achondrites, aubrites Norton County (109 Ma) and Mayo Belwa (117 Ma) and howardite Lohawat (110 Ma) have comparable exposure ages (Lorenzetti et al. 2001; Sisodia et al. 2001). In the noble gas compilation (Schultz and Franke 2000), we could only find the Antarctic chondrite Y-74035 (L6) with an exposure age (~100 Ma) similar to that of Devgaon.

Trapped Component

Trapped He and Ne are negligible, while considerable amounts of trapped ^{36}Ar, ^{84}Kr, and ^{132}Xe are present (Table 6b). This indicates that the carrier of trapped noble gases mostly contains Ar, Kr, and Xe. Phase Q fits this description well (Busemann et al. 2000). Trapped ^{84}Kr and ^{132}Xe fall in the range of values expected for petrologic type 4 (Schultz et al. 1990). The elemental ratios $(^{36}Ar/^{132}Xe) = 53.6$ and $(^{84}Kr/^{132}Xe) = 0.85$ fall in the typical range for ordinary chondrites (Busemann et al. 2000). The measured isotopic ratios of Kr and Xe corrected for spallation contribution and the values for those isotopes where no (n, γ) or radiogenic contributions are expected are as follows: $^{86}Kr/^{84}Kr$ = 0.3122 (0010) and ^{124}Xe:^{130}Xe:^{131}Xe:^{132}Xe:^{134}Xe:^{136}Xe = 0.469 (007):16.25 (04): 82.13 (10):100:37.85 (05):31.55 (07), in agreement with those observed in ordinary chondrites (Buseman et al. 2000).

Halogen Contents and Neutron Fluence

From the radiogenic $^{129}Xe^*(^{129}I) = 338.5 \times 10^{-12}$ ccSTP/g, we can estimate the I content of Devgaon, assuming the canonical value of $(^{129}I/^{127}I) = 10^{-4}$ and that all I is correlated with ^{129}I. Considering the fact that the K-Ar age is close to 4.6 Ga and the good correlation of ^{128}Xe and ^{129}Xe (Fig. 7), these assumptions look reasonable. In this way, we obtain I = 19.2 ppb. This value seems to be a factor of two to three lower than that found in other H chondrites. For example the chondrite Kesen (H4) has 60 ppb I (Dreibus et al., 1979). From the ratio $(^{82}Kr/^{128}Xe)_n$ = 32, we can also derive the Br content. We obtain a value of Br = 1.30 ppm or 2.5 ppm if neutrons are predominantly epithermal. $(Br/I)_{atom}$ ~107 (215 for epithermal neutrons) is about 18 times higher than the average value of 6 in H chondrites. Similarly, we obtain a Cl content of 403 ppm (775 ppm for epithermal neutrons), with the assumption that the $(Cl/Br)_{atom}$ ratio in Devgaon is ~700 as normally expected in H chondrites (Dreibus et al. 1979). This Cl content is about an order of magnitude higher compared to the ordinary chondrite range of 15–177 ppm (Garrison et al. 2000). Thus, we find that compared to average H chondrites (Mason 1979), Devgaon is significantly enriched in Cl and Br and depleted in I. In Table 7, the ratios of I/Cl and Br/Cl of Devgaon are compared with Kesen (H4) (a normal H chondrite), Zag (H3) (a chondrite having halites), and CI chondrites. It can be seen that while the Br/Cl values are the same within a factor of three for all samples, I/Cl ratios are different. While Kesen, CI, and Zag (matrix) values are comparable, Devgaon has about 10 times lower I/Cl. This low value cannot be accounted for by the uncertainties involved in deriving this ratio since they can, at most, make a difference of a factor of two. We, therefore, conclude that Devgaon has Cl and Br enriched by about an order of magnitude, while I is deficient by about a factor of three as compared to the average H chondrite. Halogen ratios in Devgaon are similar to those observed for Zag (halite), having a low I/Cl ratio indicating that a halogen-rich phase (probably a halite) may be present in Devgaon. It has been suggested (Whitby et al. 2000) that I deficit is expected in halite formation by brine evaporation, during which process I is largely excluded from the halite lattice. The above discussion calls for a search of halites and accurate measurement of halogens in Devgaon.

The neutron fluence to which the meteorite has been exposed can be calculated from $^{128}Xe_n$ and the I content using the relation:

$$(^{128}Xe_n) = (^{127}I) \langle \sigma_{127}\Phi_n \rangle$$

where the term $\langle \sigma_{127}\Phi_n \rangle$ is the energy-averaged product of the neutron capture cross section on ^{127}I and the neutron fluence. Inserting the values of $^{128}Xe_n$ and ^{127}I, we get $\langle \sigma_{127}\Phi_n \rangle = 1.10 \times 10^{-7}$.

For a predominantly thermal spectrum, σ_{127} = 5.5b, and we get $\Phi_n = 2.0 \times 10^{16}$ n cm^{-2} or a flux of 6.3 n cm^{-2} s^{-1} during the 101 Ma cosmic ray exposure of Devgaon. However, if the neutron spectrum is taken to be epithermal, Φ_n (30–300eV) = 8.5×10^{14} n cm^{-2}, and the flux is estimated to be 0.26 n cm^{-2} s^{-1}. The neutron flux calculated for Devgaon falls in the range of values observed in other stone meteorites based on neutron capture efects on Cl, Ca, Sm, and Gd (Bogard et al. 1995; Hidaka et al. 2000).

For a stone meteorite of ~50 cm radius, an integrated neutron flux of ~2 cm^{-2} s^{-1} has been theoritically estimated, at a depth of ~5 cm from the surface, using lunar sample data (Spergel et al. 1986). This results in a neutron fluence of 6 × 10^{15} ncm^{-2} in 100 Ma. Our sample with $(^{22}Ne/^{21}Ne)$ = 1.182, corresponding to a sample depth of ~5 cm in an object of 50 cm radius, yields a neutron fluence between (0.85–20) × 10^{15} ncm^{-2}, depending on the choice between pure epithermal or thermal spectrum, and is in reasonable agreement with the theoritical estimate. Considering the observed value of $(^{80}Kr/^{82}Kr)_n$ = 2.44, the neutron spectrum appears to be closer to epithermal range or probably is a mixture of thermal and epithermal components.

Meteoroid Size

We can calculate the minimum pre-atmospheric radius (R_{min}) of the meteoroid following the method developed by Eberhardt et al. (1963), which has also been applied in the case of martian meteorites (Eugster et al. 2002) and for the Kobe meteorite (Takaoka et al. 2002). The slowing down

Table 7. Comparision of estimated halogen ratios of Devgaon with other chondrites.[a]

Sample	$(I/Cl)_{atom}$	$(Br/Cl)_{atom}$	Reference
Devgaon (H3.8)	1.3×10^{-5}	1.43×10^{-3}	This study
Kesen (H4)	1.86×10^{-4}	1.8×10^{-3}	(1)
CI Chondrite	4.7×10^{-4}	2.1×10^{-3}	(2)
Zag (H3)			
Matrix	3.5×10^{-4}	7.6×10^{-3}	(2)
Halite	$(0.4–5.1)\ 10^{-8}$	9×10^{-4}	(2)

[a](1) Dreibus et al 1979; (2) Whitby et al. (2000).

density (q) for epithermal neutrons, defined by the number of neutrons (cm^{-3} s^{-1}) per volume and time, that were slowed down below a certain energy, is given by

$$q = \phi_n(30\text{–}300 \text{ eV}) \times \xi\Sigma_{tot} \quad (1)$$

where ξ is the average logarthmic energy decrement per collision, and Σ_{tot} is the macroscopic total cross section. For ordinary chondrites, Eberhardt et al. (1963) have calculated $\xi\Sigma_{tot}$ = 0.0354 cm^{-1}. Hence, for Devgaon, we obtain q = 0.0092 cm^{-3} s^{-1}.

Assuming a spherical shape for the meteoroid, Eberhardt et al. (1963) have obtained the following relation:

$$R_{min} = R_0 + aq \quad (2)$$

where R_0 is 22 cm, the radius below which $^{80}Kr_n$ is too small to be observed, and the parameter a is 118 cm^4 s. Since the sample used for measurement may be located close to the meteoroid surface, the epithermal neutron flux, which is strongly depth dependent, the preatmospheric size so obtained (Equation 2) is a lower limit. Thus, we get R_{min} ~23 cm for Devgaon. Taking its density as 3.5 gcm^{-3}, a minimum pre-atmospheric mass of 180 kg is estimated from the epithermal neutron slowing density. Later on, we will compare the size of the meteoroid with estimates based on track density and other isotopic measurements.

NUCLEAR TRACKS AND COSMOGENIC RADIONUCLIDES

The track density in the meteorite was measured in four spot samples taken from diagonally opposite corners and a sample from the center of the basal face. Tracks in the olivine grains were developed by etching with the WN solution (a mixture of 40% EDTA + 1% oxalic acid and orthophosphoric acid, made to pH 8.0 by adding NaOH) for 5 hr (Krishnaswami et al. 1971). The data are presented in Table 8. It is found that the track density varies between 4.6 to 9 × $10^6/cm^2$, showing a small gradient within the meteorite. Correcting for the poor sensitivity of olivines (by a factor of 2.1) and using the calculated track production rates of Bhattacharya et al. (1973) for the feldspar group of minerals, we get ablation of about 4.9 to 7.8 cm on various faces of the recovered fragment, assuming an exposure age of 101 Ma. The shielding depth derived from the track production rate is found to be in agreement with the observed high $(^{22}Ne/^{21}Ne)_c$ ratio, which implies a shielding of about 5 cm. The limited track data do not allow us to determine whether the meteoroid suffered symmetric or asymmetric ablation. Measurement of the track profile in a core through the meteoroid may enable us to ascertain the type of ablation suffered by the meteoroid.

The meteorite was quickly recovered and was available to us within 12 days after the fall. Therefore, several short-lived nuclides like ^{52}Mn (5.6 d), ^{48}V (16 d), and ^{51}Cr (27 d) could be measured using a low background, high purity, large germanium (400 cm^3) gamma ray spectrometer located in a 20 cm-thick lead shield (Shukla et al. 2001). In addition, all the long-lived gamma emitting radionuclides, e.g., ^{26}Al, ^{60}Co, ^{22}Na, ^{54}Mn, ^{57}Co, ^{46}Sc, ^{56}Co, ^{58}Co, and ^{7}Be were measured. Two samples of the meteorite were counted in this manner. An amount of 57.14 g taken from an edge of the meteorite was counted in a standard geometry, and the remaining whole rock ~3.0 kg was counted by placing it in contact with the germanium detector. The first set of measurements enabled us to measure the cosmogenic radionuclides ^{22}Na, ^{26}Al, and ^{54}Mn besides the inherent ^{40}K. Potassium concentration was determined to be 786 ppm, consistent with AAS measurements (Table 2).

The second set of measurements were used to determine the activity of all the cosmogenic radionuclides using ^{40}K (K = 804 ppm; Table 2) as an internal standard following the procedure of Bhandari et al. (1989). The measured activities are given in Table 9. The activity of ^{60}Co (<0.3 dpm/kg), which is mainly produced by the capture of thermal neutrons, suggests a low shielding depth of the recovered fragment. However, in heavy rare gases (Kr and Xe), large neutron effects have been observed. These data together imply that the meteoroid was exposed as a large body for most of its journey in space and as a small object during the last phase of its exposure, at least when ^{60}Co was produced. Since ^{26}Al (57.6 dpm/kg; Table 9) is close to its saturation value, the second stage of its exposure could be about a million years. Measurements of the longer lived radioisotopes (^{10}Be, ^{53}Mn) should enable us to determine the period of the second stage more precisely.

The Devgaon meteorite fell in February 2001, about 7

Table 8. Track density variation in the Devgaon chondrite.

Sample[a]	Track density per cm^2 (# of tracks)	Track production rate per cm^2 Ma[b]	Mean shielding depth (cm)
D-1	8.99 × 10^6 (1357)	1.9 × 10^5	4.9
D-2	8.11 × 10^6 (1969)	1.7 × 10^5	5.3
D-3	7.25 × 10^6 (915)	1.5 × 10^5	5.6
D-4	4.55 × 10^6 (1395)	9.5 × 10^4	7.8
D-5	8.13 × 10^6 (1266)	1.7 × 10^5	5.6
Random	4.56 × 10^6 (561)	9.5 × 10^4	7.8
Random	6.08 × 10^6 (908)	1.2 × 10^5	5.4

[a]Olivine grains separated from these samples are used for track studies.
[b]Track densities have been corrected for poor sensitivity of olivine by multiplying with 2.1.

Table 9. Activity of various cosmogenic radioisotopes at the time of the fall (February 12, 2001), measured in the Devgaon (H3.8) chondrite.

			Devgaon				Torino (H6)	Fermo (H)
		Energy	SET-I (box) 57.1366 g		SET-II (main mass) ~3.8 kg		(May 1988)	(25 Sept. 1996)
Isotope	Half-life	(keV)	cpm	dpm/kg	cpm	dpm/kg	dpm/kg[a]	dpm/kg[b]
^{52}Mn	5.6 d	744.5			0.35 ± 0.06	11.3 ± 2.1	20.3 ± 1.8	–
		1434.5			0.26 ± 0.04	11.6 ± 1.8		
^{48}V	16 d	983.5			0.35 ± 0.02	10.8 ± 0.67	20.8 ± 1.5	28 ± 2
		1311.6			0.28 ± 0.02	12.8 ± 0.92		
^{51}Cr	27.2 d	320.07			0.13 ± 0.013	28.5 ± 2.2	76 ± 7	88 ± 7
^{7}Be	53.3 d	477.56			0.14 ± 0.007	33.1 ± 1.7	59 ± 6	79 ± 2
^{58}Co	70.78 d	810.75			0.12 ± 0.005	3.70 ± 0.15	11 ± 0.7	10.9 ± 0.2
^{56}Co	78.8 d	846.75			0.12 ± 0.005	3.66 ± 0.15	7.7 ± 0.75	7.9 ± 0.2
^{46}Sc	83.9 d	889.26			0.15 ± 0.005	4.84 ± 0.16	10.4 ± 2	11.8 ± 0.2
^{57}Co	271.35 d	122.07			0.23 ± 0.003	5.13 ± 0.07	16.3 ± 1	13.6 ± 0.2
^{54}Mn	312.2 d	834.8	0.21 ± 0.01	72.8 ± 3.5	1.9 ± 0.01	58.9 ± 0.35	121 ± 2	114.6 ± 0.3
^{22}Na	2.6 y	1274.5	0.10 ± 0.01	50 ± 5	1.52 ± 0.01	68.0 ± 0.49	80 ± 1	86.7 ± 0.3
^{60}Co	5.27 y	1173.20			0.005 ± 0.005	0.22 ± 0.22 <0.44	2.8 ± 0.3	0.82 ± 0.06
		1332.51			0.011 ± 0.005	0.49 ± 0.22 <0.71		0.89 ± 0.06
^{26}Al	7.3×10^5 y	1809.0	0.06 ± 0.003	43 ± 0.7	0.90 ± 0.006	57.6 ± 0.38	54 ± 1.1	57.0 ± 0.3
^{40}K	1.25×10^9 y	1460.7	0.36 ± 0.008	786[c]	3.56 ± 0.01			
^{22}Na/^{26}Al				1.16		1.18	1.48	1.52

[a]Bhandari et al. (1989).
[b]Bonino et al. (2001).
[c]Corresponds to the total K concentration.

months after the solar maximum of cycle 23, which recorded the maximum monthly mean sunspot number of 170.1 in July 2000. The activities of short-lived radionuclides can be used to infer the extent of modulation of galactic cosmic rays by the solar activity. The intensity of galactic cosmic rays is anticorrelated with the sun spot number due to the accompanying changes in the intensity of the heliospheric magnetic field. The neutron monitor count rates, N_m, enable us to compute the time variation of nuclide production rates, since the nuclide production rates are directly related to the neutron monitor count rates (Bhandari et al. 1989). We have used the Climax neutron monitor data and numerically integrated the nuclide production to obtain their expected time variation over the past four decades. A small phase lag, relative to the neutron monitor count rates, occurs in the activity of radionuclides with half-life smaller or comparable to the solar cycle, depending on their half-life (Evans et al. 1982; Bhandari et al. 1989; Bonino and Castagnoli 1997) while the production of the long lived radionuclides are not affected by the solar cycle. In light of these calculations, we now discuss the salient features of the observed activity pattern of radioactivities in the Devgaon meteorite. Firstly, we compare the observed activities in Devgaon with other recently fallen H chondrites, e.g., Torino (May 1988) and Fermo (September 1996), which are almost similar in chemical composition, belong to the same petrological class (4 and 6) and fell during the phases of different solar cycles. The activities of most of the short-lived (<2.6 years) radionuclides (Table 9) in Devgaon are a factor of ~2 to 3 lower compared to Torino. The range of the ratios (0.31 to 0.48) of various radionuclides in the two meteorites can be understood in terms of the flux over the few mean lives of various isotopes, which is clearly the consequence of the magnitude of solar modulation of galactic cosmic rays before the fall of the meteorite.

Although ^{22}Na/^{26}Al is identical in the first and second sets, ^{54}Mn/^{22}Na is different, 1.4 and 0.9 respectively. Since major contributions to ^{22}Na and ^{26}Al come from similar nuclear reactions, i.e., (n, p2n) on ^{24}Mg and ^{28}Si, respectively and smaller contributions from (n, 2n) on ^{23}Na and ^{27}Al, respectively, the ^{22}Na/^{26}Al production ratio is nearly independent of shielding depth. ^{54}Mn/^{22}Na is sensitive to shielding depth, having significant production at higher depths (where neutron fluence is large) for ^{54}Mn. This is because of the additional contribution from the 5.8% abundant ^{54}Fe(n, p) reaction, apart from ^{56}Fe(n, p2n) and ^{55}Mn(n, 2n) reactions. The cross section of the (n, p) reaction is relatively much higher than those of the (n, p2n) and (n, 2n) reactions. On comparing these values with their production profiles, we find that this ratio is consistent with shielding depths of <25 cm. The ^{22}Na/^{26}Al ratio in Devgaon (1.18 ± 0.01) is among the lowest values found in chondrites and is about 18% lower than the expected value (1.44) at the time of fall of the meteorite. The ratio ^{22}Na/^{26}Al is an indicator of the integrated fluxes of cosmic rays during the 4 to 5 yr before the fall of the meteorite, and such low values are generally found in chondrites, which fall immediately after a solar maximum.

The low ^{22}Na/^{26}Al ratio in meteorites can occur in two ways. A complex exposure due to fragmentation in space within the past 1 Ma will still have some ^{26}Al surviving from the previous exposure as a large body (40–50 cm) and could result in ^{22}Na/^{26}Al lower than expected. Thus, a recent

(<1 Ma) fragmentation occurred in space, changing the meteorite from a large (50 cm) to a small (20–25 cm) body, based on production rates of Bhandari et al. (1993) and Leya et al. (2000). Alternatively, such values can result from lower cosmic ray flux in the recent past compared to their long-term fluxes. A slow decrease in cosmic ray fluxes over the past century (by a factor of two) has been inferred from the increase in heliospheric magnetic field (Lockwood et al. 1999; Solanki et al. 2000; Bonino et al. Forthcoming), and this effect has also been observed in ^{22}Na and ^{44}Ti measured in some recently fallen meteorites (Bhandari et al. 2002; Ghosh et al. 2002; Bonino et al. 2001). As mentioned before, measurements of longer lived radionuclides may help resolve these two alternatives.

EXPOSURE SCENARIO FOR DEVGAON

Different cosmogenic effects, i.e., heavy nuclei tracks, (^{22}Ne/^{21}Ne), neutron capture isotopes (^{60}Co, ^{36}Ar, $^{80,\,82}$Ke, ^{128}Xe), and other radionuclides are sensitive to shielding depths at different time and depth scales (from centimeters to meters), and thus, their measurements allow us to construct the exposure history of the meteoroid. Various cosmogenic products studied in the Devgaon meteorite are all consistent with the small shielding depth of the recovered fragment. Evidence for a complex exposure comes from the disagreement of thermal and epithermal neutron fluence calculated on the basis of ^{36}Ar$_n$, ^{82}Kr$_n$, and ^{128}Xe$_n$ on the onehand and the very low activity of ^{60}Co on the other (Table 10). A breakup of a large fragment (~50 cm) in the recent past (within one half-life of ^{26}Al), resulting in a fragment that is the current meteoroid (25 cm), is consistent with the observed cosmogenic effects. The current meteoroid fragment might be close to the surface of the pre-breakup object, as is indicated by low shielding from the (^{22}Ne/^{21}Ne)$_c$ value. Thus, the various cosmogenic effects put several constraints on the exposure history and sizes of the meteoroid and the shielding depth of the sample analyzed from this meteorite, which has one of the largest exposure ages of 101 Ma. In view of these data, we may conclude that a body of about 50 cm radius was exposed in the interplanetary space for nearly 100 million years, when neutron effects in Cl, Br, and I produced excess ^{36}Ar, $^{80,\,82}$Kr, and ^{128}Xe (stage I), and then broke into a smaller body (~23 cm radius) about a million years ago where all the observed radioisotopes, including ^{60}Co, were produced (stage II). The recovered fragment contained material that was exposed at a low shielding depths (<5 cm) in both stages II and I, where heavy nuclear tracks and cosmogenic neon were produced for 101 Ma. The observed data do not require any significant irradiation on the parent body of the meteoroid before stage I.

Acknowledgments–We thank the collector, Bastar, for his help in obtaining the meteorite sample. Help provided by Dr. Clifford Lopate at the University of New Hampshire for the Climax/Haleakala neutron monitor data and funded by the NSF grant ATM 99–12341 is appreciated. Thanks are due to U. Heitmann and T. Grund (Münster) for thin section preparation and technical assistance, respectively. Critical reviews by K. Nishiizumi and an annonymous reviewer and suggestions by Associate Editor I. Lyon are greatly appreciated.

Editorial Handling—Dr. Ian Lyon

Table 10. Shielding depths calculated on the basis of various tracers.

Tracer	Value	Shielding depth
Tracks	~10^5/cm^2	4.8–7.8 cm
(^{22}Ne/^{21}Ne)$_c$	1.182 ± 0.001	≤5 cm
^{60}Co	<0.3 dpm/kg	<20 cm
^{26}Al	57.6 dpm/kg	20–60 cm
(^{80}Kr/^{82}Kr)$_n$	2.44	≥23 cm
^{128}Xe$_n$	0.373×10^{-12} cc STP/g	≥23 cm

REFERENCES

Bhandari N., Bonino G., Callegari E., Castagnoli G. C., Mathew K. J., Padia J. T., and Queirazza G. 1989. The Torino, H6 meteorite shower. *Meteoritics* 24:29–34.

Bhandari N., Mathew K. J., Rao M. N., Herpers U., Bremer K., Vogt S., Wilfli W., Hofmann H. J., Michel R., Bodemann R., and Lange H. J. 1993. Depth and size dependence of cosmogenic nuclide production rates in stony meteoroides. *Geochimica et Cosmochimica Acta* 57:2361–2376.

Bhandari N., Murty S. V. S., Shukla P. N., Shukla A. D., Mahajan R. R., Sarin M. M., Srinivasan G., Suthar K. M., Sisodia M. S., Jha S., and Bischof A. 2002. Itwa Bhopji (L3/5) chondrite regolith breccia: Fall, classification, and cosmogenic records. *Meteoritics & Planetary Science* 37:549–563.

Bhattachraya S. K., Goswami J. N., and Lal D. 1973. Semiempirical rates of formation of cosmic ray tracks in spherical objects exposed in space: Preatmospheric and post atmospheric depth profiles. *Journal of Geophysical Research* 78:8356–8363.

Bischoff A. and Keil K. 1983. Catalog of Al-rich chondrules, inclusions and fragments in ordinary chondrites. *Special Publication No. 22.* Albuquerque: University of New Mexico, Institute of Meteoritics. pp. 1–33.

Bischoff A. and Keil K. 1984. Al-rich objects in ordinary chondrites: Related origin of carbonaceous and ordinary chondrites and their constituents. *Geochimica et Cosmochimica Acta* 48:693–709.

Bogard D. D., Nyquist L. E., Bansal B. M., Garrison D. H., Wiesman H., Herzog G. F., Albrecht A. A., Vogt S., and Klein J. 1995. Neutron-capture ^{36}Cl, ^{41}Ca, ^{36}Ar, and ^{150}Sm in large chondrites: Evidence for high fluence of thermalized neutrons. *Journal of Geophysical Research* E5:9401–9416.

Bonino G. and Castagnoli G. C. 1997. Solar cycles recorded in meteorites. In *Past and present variability of the solar-terrestrial system: Measurement, data analysis, and theoretical models,* edited by Castagnoli G. C. and Provenzale A. Amsterdam: IOS Press. 491 p.

Bonino G., Bhandari N., Murty S. V. S., Mahajan R. R., Suthar K. M., Shukla A. D., Shukla P. N., Cini Castagnoli G., and Taricco C. 2001. Solar and galactic cosmic ray records of the Fermo (H) chondrite regolith breccia. *Meteoritics & Planetary Science* 36: 831–839.

Bonino G., Cini Castagnoli G., Cane D., Taricco C., and Bhandari N. Forthcoming. Increase in the galactic cosmic ray flux during prolonged solar quiet periods: Validation by measurement of cosmogenic ^{44}Ti in meteorites. *Advances in Space Research.*

Busemann H., Baur H., and Wieler R. 2000. Primordial noble gases in "phase Q" in carbonaceous and ordinary chondrites studied by closed-system stepped etching. *Meteoritics & Planetary Science* 35:949–973.

Dreibus G., Spettel B., and Wänke H. 1979. Halogens in meteorites and their primordial abundances. In *Origin and distribution of elements,* edited by Ahrens L. H. New York: Pergamon Press. pp 33–38.

Eberhardt P., Geiss J., and Lutz H. 1963. Neutrons in meteorites. In *Earth science and meteoritics,* edited by Geiss J. and Goldberg E. D. Amsterdam: North Holland Publishing Comapny. pp. 143–168.

Eugster O. 1988. Cosmic ray production rates for ^{3}He, ^{21}Ne, ^{38}Ar, ^{82}Kr, and ^{126}Xe in chondrites based on ^{81}Kr-Kr exposure ages. *Geochimica et Cosmochimica Acta* 52:1649–1662.

Eugster O., Busemann H., Lorenzetti S., and Terribilini D. 2002. Ejection ages from krypton-81-krypton-83 dating and pre-atmospheric sizes of martian meteorites. *Meteoritics & Planetary Science* 37:1345–1360.

Evans J. C., Reeves J. H., Rancitelli L. A., and Bogard D. D. 1982. Cosmogenic nuclides in recently fallen meteorites: Evidence for galactic cosmic ray variations during the period 1967–1978. *Journal of Geophysical Research* 87:5577–5591.

Garrison D., Hamlin S., and Bogard D. 2000. Chlorine abundances in meteorites. *Meteoritics & Planetary Science* 35:419–429.

Ghosh S., Murty S. V. S., Pant N. C., Ghosh J. B., Shome S., Shukla A. D., Mahajan R. R., Shukla P. N., and Bhandari N. 2002. Fall, classification, and cosmogenic records of the Sabrum (LL6) chondrite. *Meteoritics & Planetary Science* 37:439–448.

Göebel R., Begemann F., and Ott U. 1982. On neutron induced and other noble gases in Allende inclusions. *Geochimica et Cosmochimica Acta* 46:1777–1792.

Hidaka H., Ebihara M., and Yoneda S. 2000. Isotopic study of neutron capture effects on Sm and Gd in chondrites. *Earth and Planetary Science Letters* 180:29–37.

Hintenberger H., Schultz L., and Wänke H. 1966. Messung der diffusionverluste von radiogenen und spallogenen edlegassen in steinmeteoriten II. *Zeitschrift für Naturforschung* 19A:1147–1159.

Hohenberg C. M., Hudson B., Kennedy B. M., and Podosek F. A. 1981. Xenon spallation systematics in Angra Dos Reis. *Geochimica et Cosmochimica Acta* 45:1909–1915.

Kallemeyn G. W., Rubin A. E., Wang D., and Wasson J. T. 1989. Ordinary chondrites bulk composition, classification, lithophile element fractionations and composition-petrographic type relationships. *Geochimica et Cosmochimica Acta* 53:2247–2267.

Krishnaswami S., Lal D., Prabhu M., and Tamhane A. S. 1971. Olivine: Revelation of tracks of charged particles. *Science* 174: 287–291.

Laul J. C. 1979. Neutron activation analysis of geological materials. *Atomic Energy Review* 17:603–695.

Lavielle B. and Marti M. 1988. Cosmic ray-produced Kr in St. Severin core A III. Proceedings, 8th Lunar and Planetary Science Conference. pp. 565–572.

Leya I., Lange H. J., Neumann S., Wieler R., and Michel R. 2000. The production of cosmogenic nuclides in stony meteoroids by galactic cosmic ray particles. *Meteoritics & Planetary Science* 35:259–286.

Lockwood M., Stamper R., and Wild M. N. 1999. A doubling of the Sun's coronal magnetic field during the past 100 years. *Nature* 399:437–439.

Lorenzetti S., Eugster O., Burbine T., McCoy T., and Marti K. 2001. Break-up events on the aubrite parent body. *Meteoritics & Planetary Science* 36:A116–A117.

Marti K. Eberhardt P., and Geiss J. 1966. Spallation, fission, and neutron capture anomalies in meteoritic krypton and xenon. *Zeitschrift für Naturforschung* 21a:398–413.

Marti K. and Graf T. 1992. Cosmic say exposure history of ordinary chondrites. *Annual Review of Earth and Planetary Sciences* 20: 221–243.

Mason B. 1979. Cosmochemistry, Part 1, Meteorites. In *Data of geochemistry,* edited by Fleischer F. Professional Paper 440-B-1. Washington D.C.: U.S. Geological Survey. pp. B1–B132.

Murty S. V. S. 1997. Noble gases and nitrogen in Muong Nong tektites. *Meteoritics* 32:687–691.

Murty S. V. S., Bhandari N., Suthar K. M., Clement C. J., Bonino G., and Castagnoli G. C. 1998. Cosmogenic effects in Mbale, L5/6 chondrite. *Meteoritics & Planetary Science* 33:1311–1316.

Schultz L., Weber H. W., and Begemann F. 1990. Planetary noble gases in H3 and H4 chondrite falls. *Meteoritics* 25:405–406.

Schultz L. and Franke L. 2000. *Helium, neon, and argon in meteorites—A data compilation.* CD-ROM. Mainz: Max-planck-Institut für Chemie.

Shukla A. D., Adhyaru P., and Bhandari N. 2001. Highly sensitive γ-γ coincidence/anticoincidence spectrometer for measurement of low radioactivity in meteorites. In *Proceedings of Symposium on nuclear analytical and radiochemistry.* Mumbai: Bhabha Atomic Research Center. pp. 554–555.

Sisodia M. S., Shukla A. D., Suthar K. M., Mahajan R. R., Murty S. V. S, Shukla P. N., Bhandari N., and Natrajan R. 2001. The Lohawat howardite: Mineralogy, chemistry, and cosmogenic effects. *Meteoritics & Planetary Science* 36:1457–1466.

Solanki S. K., Schüssler M., and Figge M. 2000. Evolution of the Sun's large-scale magnetic field since the Maunder minimum. *Nature* 408:445–447.

Spergel M. S., Reedy R. C., Lazareth O. W., Levy P. W., and Slatest L. A. 1986. Cosmogenic neutron-capture-produced nuclides in stony meteorites. *Journal of Geophysical Research* 91:D483–D494.

Stöffler D., Keil K., and Scott E. R. D. 1991. Shock metamorphism of ordinary chondrites. *Geochimica et Cosmochimica Acta* 55: 3845–3867.

Takaoka N., Nakamura T., Nagao K., and Nakamura N. 2002. Noble gases in the Kobe CK4 carbonaceous chondrite. *Geochemical Journal* 36:355–368.

Wasson J. T. and Kallemeyn G. W. 1988. Composition of chondrites. *Philosophical Transactions of the Royal Society of London A* 325:535–544.

Whitby J., Burgess R., Turner G., Gilmour J., and Bridges J. 2000. Extinct 129I in Halite from a primitive meteorite: Evidence for evaporite formation in the early solar system. *Science* 288:1819–1821.

Wieler R., Graf T., Signer P., Vogt S., Herzog G. F., Tuniz C., Fink D., Fifield L. K., Klein J., Middleton R., Jull A. J. T., Pellas P., Masarik J., and Dreibus G. 1996. Exposure history of the Torino meteorite. *Meteoritics & Planetary Science* 31:265–272.